

EFFECTS OF SHEAR-FRACTURE DISPLACEMENT AND ORIENTATION ON FRACTURE TOPOLOGY AND ABSOLUTE PERMEABILITY

Sultan Al Enezi
Abraham Grader (Penn. State University)
Phillips Halleck

This paper was prepared for presentation at the International Symposium of the Society of Core Analysts held in Calgary, Canada, 10-12 September, 2007

ABSTRACT

Four dry Berea samples (25 mm diameter, 70 mm long) were fractured under shear in a Hoek cell (1500 psig confining) and then scanned with high-resolution CT (voxel dimensions 0.030 mm x 0.030 mm x 0.033 mm) in order to study fracture topology and its effects on absolute permeability. Two of the samples were cut perpendicular to bedding and two were cut parallel to bedding. After peak stress two samples (one perpendicular to bedding and one parallel to bedding) were displaced by 0.2 mm at constant displacement rate (0.003 mm/sec). The other two remaining samples were not subjected to additional displacement after the peak stress. Nitrogen Klinkenberg permeabilities were measured on all four samples before and after fracturing. The shear fracture macro-porosity was extracted from the CT data.

Overall, the presence of the fracture increased the absolute permeability between 19% and 110% in the specific cases for this study. The macro-volume of the fracture in the perpendicularly layered sample is larger and more connected than the fracture volume in the parallel-layered case. Increasing the fracture displacement distance reduced the overall macro-porosity volume indicating the enlargement of the asperity areas and increasing the fracture gouge. In the parallel case, increasing the fracture displacement increased the connectivity of the fracture and its absolute permeability (relative to the non-displaced case). In the perpendicular case, fracture displacement reduced the connectivity and its absolute permeability. The fractures in the perpendicular case are more connected than the parallel case as observed in three-dimensional renderings of the fractures.

The data presented in this paper will provide opportunities for multi-phase flow studies in controlled and well-characterized shear-fracture geometries.

INTRODUCTION

Many hydrocarbon reservoirs are naturally fractured. Fluid flow patterns and hydrocarbon recovery are greatly affected by the fractures. Fractures can have positive effects on the recovery process by increasing the permeability, but may also have negative effects when they form bypass paths, especially in production-injection systems. Injected fluid may preferentially flow through the fractures leaving behind inaccessible hydrocarbons thus increasing the residual oil saturation. Fractures can also act as no-flow

reservoir boundaries. Many papers in the literature have discussed single and multi-phase flow in tensile fracture but very little discussed the shear fracture. Makurat *et al.* (1985) studied the effects of shear deformation on the permeability of natural rough joints. The experimental results showed significant increase in the conductivity with shear displacement. However when Tuefel (1987) investigated the effects of shear deformation on the permeability of fractured rocks, he found that the permeability decreased with increased shear deformation. Mohammad (2004) studied the effect of shear fracture on absolute permeability in sandstone samples cut perpendicular to bedding plane, the results showed that the permeability increased about 80% after fracturing. Al Enezi (2005) studied the effect of shear fracture induced diagonally with the bedding plane; the results showed a reduction of the absolute permeability after fracturing. All above studies were done with single phase flow and their results are not consistent and did not discuss the relationship between fracture morphology and flow behavior.

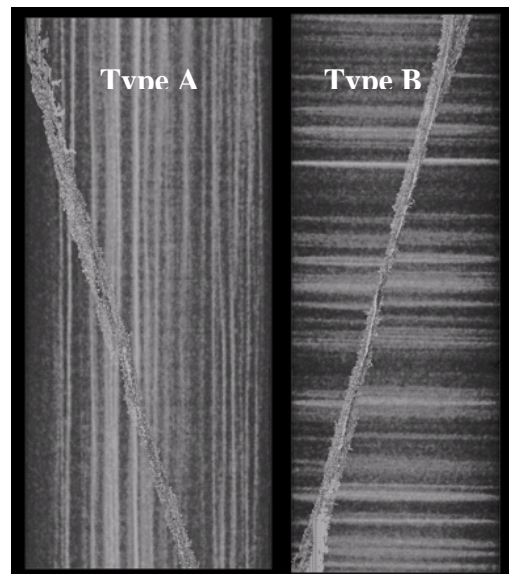
The objective of this study is to address the absolute permeability behavior of Berea sandstone samples and to correlate with the fracture morphology under different degrees of shear displacement.

PROCEDURE

Four cylindrical samples of Berea Sandstone (25 mm diameter by 70 mm long) were cut parallel to bedding planes (type A) and perpendicular to bedding planes (type B). Samples were fractured dry in triaxial compression in a stiff testing machine at 10.3 MPa confining pressure at a displacement rate of 0.003 mm/sec. Figure 1 shows an example of the resultant shear fractures. After peak stress, two samples (one type A and one type B) were displaced by 0.2 mm. The other remaining samples were not subjected to additional displacement after the peak stress. Nitrogen Klinkenberg permeabilities were measured for all the samples before and after fracturing under a confining stress of 10.3 MPa.

The samples were scanned at ambient condition using X-ray micro CT to visualize the morphology of the fractures. CT system uses a 225 kV, 225 watt X-ray source, with a maximum resolution of 5 microns. An area detector and axial motion control allow the collection of 3-D volumetric data. We used 160 kV and 120 mA to obtain 2100 slices (voxel dimensions 0.030 mm x 0.030 mm x 0.033 mm).

Figure 1: Representation of resultant fractures in Berea Samples cut parallel to bedding planes (left) and perpendicular to bedding planes (right).



DATA ANALYSIS

Absolute Permeability

Table 1 shows the permeability values before and after fracturing as a function of the degree of displacement applied for each sample. The observations for permeability data are:

- The permeability of all samples increased after fracturing.
- The permeability in type B samples increased more than that of type A samples.
- The magnitude of the change in type A samples increased with displacement.
- However in type B the magnitude of change decreased with displacement.

Sample	Sample #	Displacement	Permeability (mD)		Change	
Type	No.	mm	Before	After	mD	%
Parallel	1A	0	56.5	67.1	10.6	19
	4A	0.2	27.4	37	9.6	35
Perpendicular	1B	0	22.4	47	24.6	110
	4B	0.2	14.1	22.6	8.5	60

Table 1: permeability values of sandstone samples cut parallel and perpendicular to bedding planes before and after fracturing.

X-ray CT Scanning Sequences

In the X-ray CT image, the fractures are identified by sub-planer features with X-ray absorption that is lower than the absorption of the rock matrix indicating increased porosity. The fracture morphology was mapped by segmenting voxels that have CT-numbers lower than the mean rock matrix CT values by a set of arbitrary threshold. Figure 2 shows the fractures created without post-fracturing displacement for samples 1A (parallel) and 1B (perpendicular). The fracture in sample 1B is well connected and the asperities area is small, while in the sample 1A, the fracture is not well connected and the asperities area is large when compared to that of sample 1B. Figure 3 summarizes the result of sample 4A and sample 4B. The fracture in both samples was displaced by 0.2 mm. The fractures in both samples are not well connected and they contain large asperity areas.

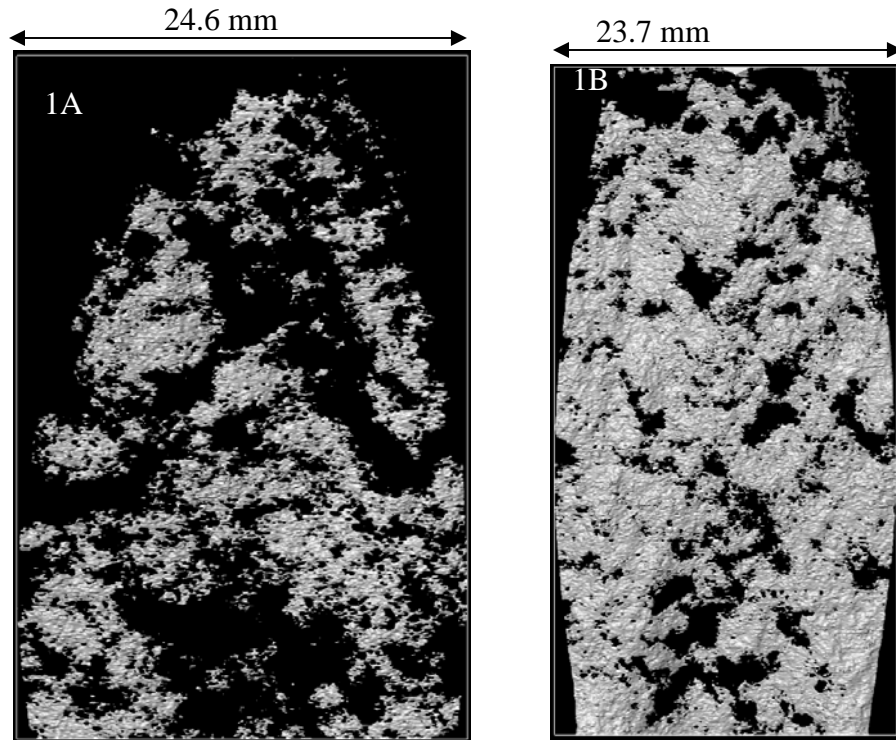


Figure 2: Fracture map of samples 1A (left, 41.3 mm) and 1B (right, 51.2 mm) without post-fracture displacement.

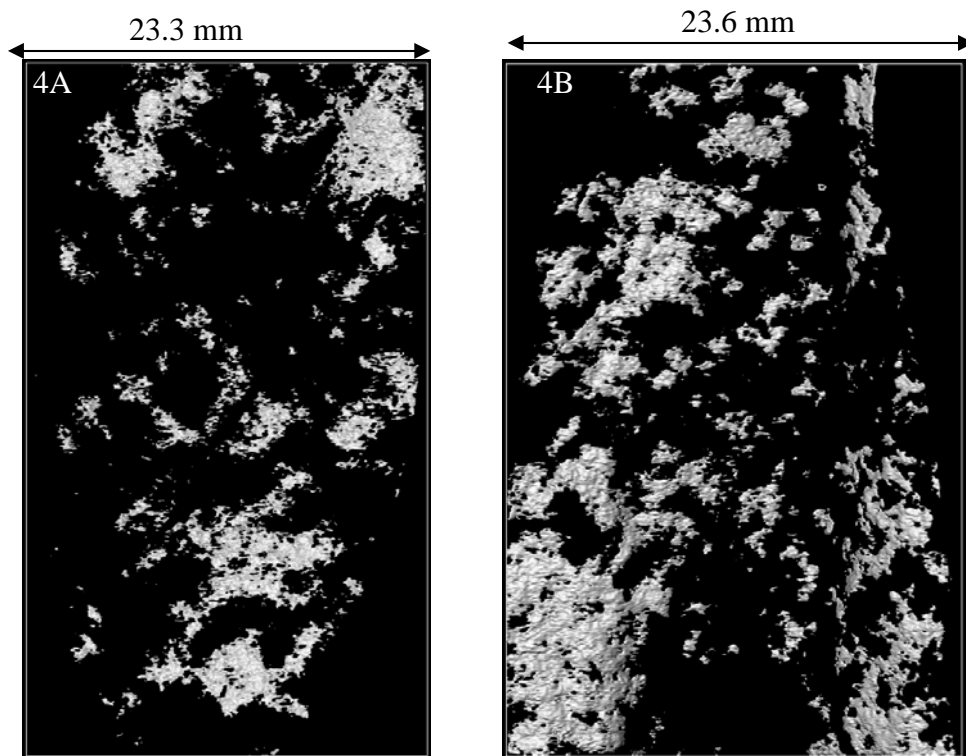


Figure 3: Fracture map of samples 4A (left, 44.6 mm) and 4B (right, 39.6 mm) with 0.2 mm post-fracture displacement.

Figure 4 shows the fracture porosity and the fracture aperture distribution for the parallel and perpendicular samples at different degrees of displacement. Samples cut parallel to bedding planes have lower fracture porosity than samples cut perpendicular to bedding planes. Post-fracturing displacement leads to lower fracture porosity than the porosity of non-displaced fracture. As the post-fracturing displacement increased, the effect of displacement on fracture aperture is greater on the perpendicular samples. Aperture distribution is consistent with fracture volume.

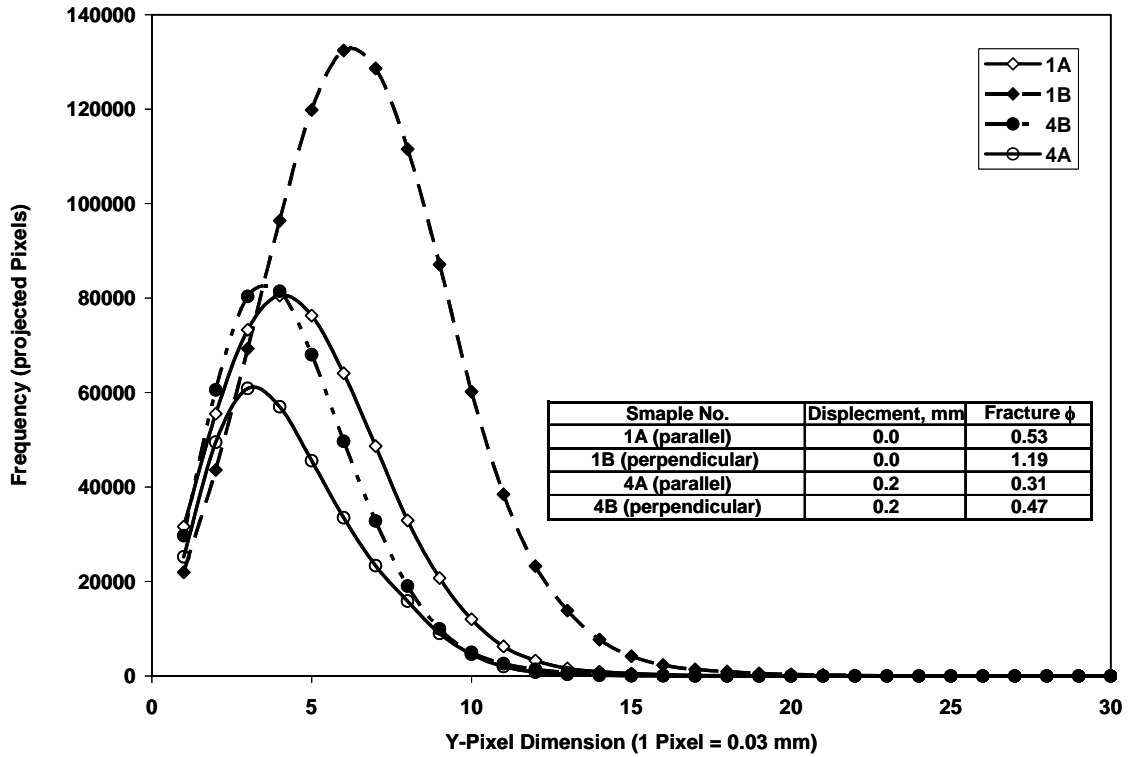


Figure 4: Aperture distribution for both types of samples (dashed lines for 0 displacement, and solid lines for 0.20 mm displacement, 1 pixel = 0.03 mm).

DISCUSSION

As the fluid reaches the fracture, it has two possible directions of flow, either across or along the fracture plane. Fluid crossing the fracture plane will either pass through void spaces or through asperities. In the former case the effect on the permeability will be negligible because the fracture width is small in comparison to the length of the sample. In the latter case the permeability could be reduced due to grinding the asperities and forming the fault gouge. The other direction will be along the fracture. The fracture plane permeability will be enhanced overall because of enhanced porosity. The results of this study shows the permeability increased after fracturing suggesting that the flow path is along the fracture.

CONCLUSION

Shear fracture leads to increased permeability of Berea Sandstone for single phase flow. The degree of displacement has an effect on absolute permeability and on the morphology of the resulted fracture. As the post-fracturing displacement increased, the fracture porosity decreased. To address the effects of shear fracture on multi-phase flow, a multiphase flow experiment using two immiscible fluids is in progress in which x-ray micro CT will be used to visualize the fluid saturation and distribution within the fracture.

ACKNOWLEDGMENTS

I gratefully acknowledge the financial support of the U.S. Department of Energy and Saudi ARAMCO. Also thanks are due to Dr. Chris Marone and his group for assistance in the fracturing process.

REFERENCES

- Al Enezi, S. “ Two Phase Flow in a Shear Fracture in a Layered Sandstone”. MS Thesis, Pennsylvania State University, 2005.
- Makurat, A. “The Effect of Shear Displacement on the Permeability of Natural Rough Joints”. Proceedings of the 17th International Congress of the International Association of Hydrogeologists, 1985. **Vol. 39**, pages 99–106.
- Mohammad, N. “Effects of Artificial Shear Fracture on Two-Phase Flow in Berea Sandstone”. MS. Thesis, Pennsylvania State University, 2004.
- Teufel, L. W. (1987). “Permeability Changes During Shear Deformation of Fractured Rock,”. Proceedings of the 28th U.S. Symposium on Rock Mechanics, 1987, **vol. 129**, pages 473–480.